CD34+ acute myeloid leukemia cells with low levels of reactive oxygen species show increased expression of stemness genes and can be targeted by the BCL2 inhibitor venetoclax

Katharina Mattes,[1] Mylène Gerritsen,[1] Hendrik Folkerts,[1] Marjan Geugien,[1] Fiona A. van den Heuvel,[1] Arthur Flohr Svendsen,[2] Guoqiang Yi,[3] Joost H.A. Martens[3] and Edo Vellenga[1]

[1]Department of Hematology, Cancer Research Center Groningen, University Medical Center Groningen, University of Groningen, Groningen; [2]Laboratory of Ageing Biology and Stem Cells, European Research Institute for the Biology of Ageing, University Medical Center Groningen, University of Groningen, Groningen and [3]Department of Molecular Biology, Faculty of Science, Radboud Institute for Molecular Life Sciences, Radboud University Nijmegen, Nijmegen, the Netherlands.

Correspondence: EDO VELLENGA - e.vellenga@umcg.nl

doi:10.3324/haematol.2019.229997

Supplementary Information

to

"CD34⁺ acute myeloid leukemia cells with low levels of reactive oxygen species show increased expression of stemness-genes and can be targeted by the BCL2 inhibitor Venetoclax"

Katharina Mattes, Mylène Gerritsen, Hendrik Folkerts, Marjan Geugien, Fiona A. van den Heuvel, Arthur Flohr Svendsen, Guoqiang Yi, Joost H.A. Martens, Edo Vellenga

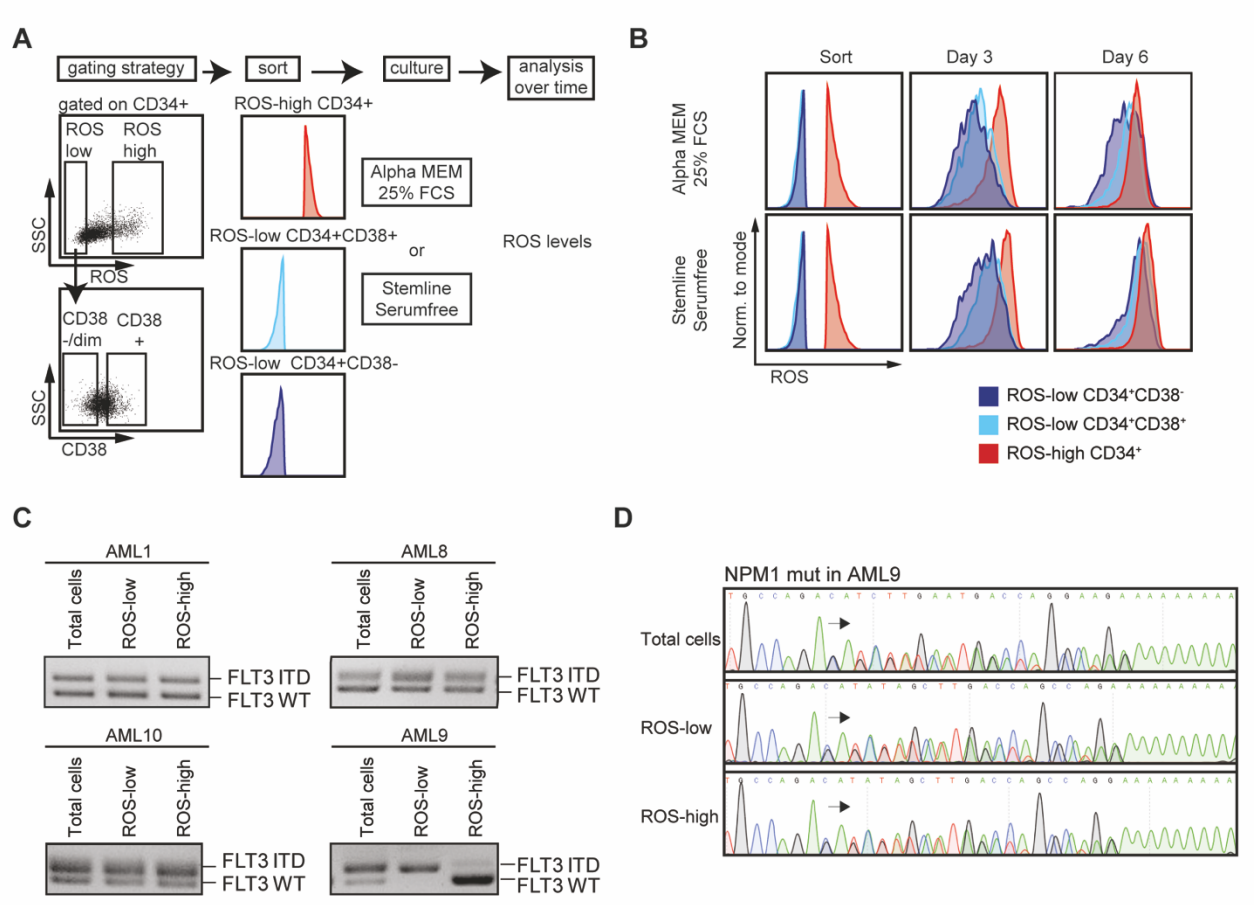

Supplementary figure 1. **ROS-low and ROS-high cells represent two distinct cell entities but both carry leukemia associated mutations (A)** Experimental design to monitor cellular ROS-states over time under different culture conditions. **(B)** FACS plots indicating ROS levels of AML cells (sorted as in A) at the time of sort and after 3 or 6 days of culture in either serum-rich medium

(upper panel) or serum-free medium (lower panel). **(C)** PCRs to detect FLT3-ITD or wildtype in total $CD34^+$ AML cell fractions, ROS-low or ROS-high sorted cells, respectively. All cell fractions of AML1, AML8 and AML10 carry both the FLT3 wildtype and FLT3-ITD allele. In AML9, the FLT3-ITD allele is only found in the ROS-low fraction. **(D)** Sequencing results verifying that the NPM1 mutation is present in all indicated cell fractions of AML9.

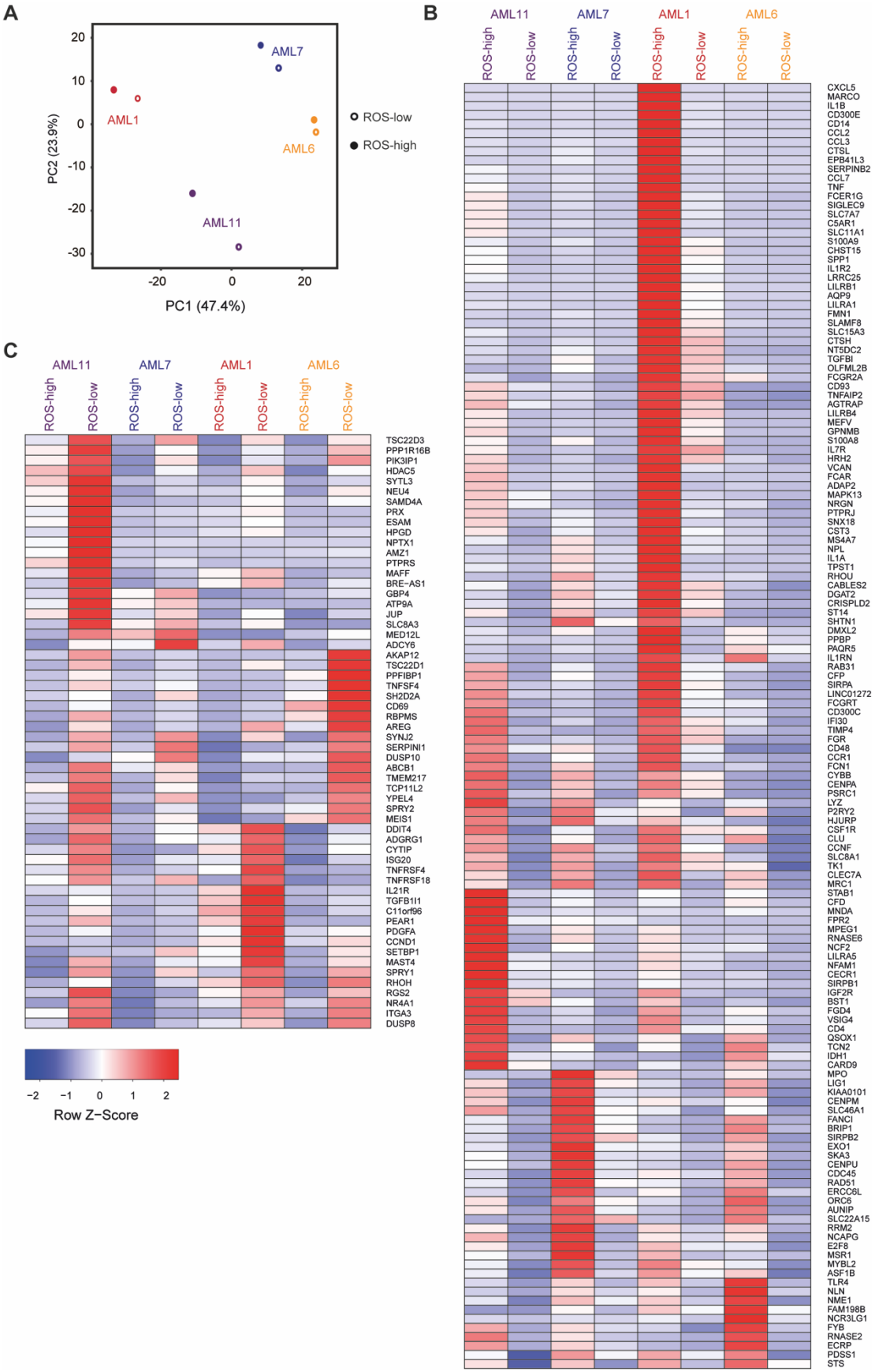
A
AML7
AML1
AML6
AML11
ROS-low
ROS-high
PC2 (23.9%)
PC1 (47.4%)
B
AML11
AML7
AML1
AML6
ROS-high
ROS-low
C
TSC22D3
PPP1R16B
PIK3IP1
HDAC5
SYTL3
NEU4
SAMD4A
PRX
ESAM
HPGD
NPTX1
AMZ1
PTPRS
MAFF
BRE-AS1
GBP4
ATP9A
JUP
SLC8A3
MED12L
ADCY6
AKAP12
TSC22D1
PPFIBP1
TNFSF4
SH2D2A
CD69
RBPMS
AREG
SYNJ2
SERPINI1
DUSP10
ABCB1
TMEM217
TCP11L2
YPEL4
SPRY2
MEIS1
DDIT4
ADGRG1
CYTIP
ISG20
TNFRSF4
TNFRSF18
IL21R
TGFB1I1
C11orf96
PEAR1
PDGFA
CCND1
SETBP1
MAST4
SPRY1
RHOH
RGS2
NR4A1
ITGA3
DUSP8
Row Z-Score
CXCL5
MARCO
IL1B
CD300E
CD14
CCL2
CCL3
CTSL
EPB41L3
SERPINB2
CCL7
TNF
FCER1G
SIGLEC9
SLC7A7
C5AR1
SLC11A1
S100A9
CHST15
SPP1
IL1R2
LRRC25
LILRB1
AQP9
LILRA1
FMN1
SLAMF8
SLC15A3
CTSH
NT5DC2
TGFBI
OLFML2B
FCGR2A
CD93
TNFAIP2
AGTRAP
LILRB4
MEFV
GPNMB
S100A8
IL7R
HRH2
VCAN
FCAR
ADAP2
MAPK13
NRGN
PTPRJ
SNX18
CST3
MS4A7
NPL
IL1A
TPST1
RHOU
CABLES2
DGAT2
CRISPLD2
ST14
SHTN1
DMXL2
PPBP
PAQR5
IL1RN
RAB31
CFP
SIRPA
LINC01272
FCGRT
CD300C
IFI30
TIMP4
FGR
CD48
CCR1
FCN1
CYBB
CENPA
PSRC1
LYZ
P2RY2
HJURP
CSF1R
CLU
CCNF
SLC8A1
TK1
CLEC7A
MRC1
STAB1
CFD
MNDA
FPR2
MPEG1
RNASE6
NCF2
LILRA5
NFAM1
CECR1
SIRPB1
IGF2R
BST1
FGD4
VSIG4
CD4
QSOX1
TCN2
IDH1
CARD9
MPO
LIG1
KIAA0101
CENPM
SLC46A1
FANCI
BRIP1
SIRPB2
EXO1
SKA3
CENPU
CDC45
RAD51
ERCC6L
ORC6
AUNIP
SLC22A15
RRM2
NCAPG
E2F8
MSR1
MYBL2
ASF1B
TLR4
NLN
NME1
FAM198B
NCR3LG1
FYB
RNASE2
ECRP
PDSS1
STS

Supplementary figure 2. **ROS-low CD34$^+$ AML cells show increased expression of genes that negatively regulated cell- proliferation and differentiation (A)** Principle component analysis (PCA) of RNA-sequencing data of indicated fractions of CD34$^+$ enriched AML cells. PC1 (x-axis) represents 47,4% and PC2 (y-axis) represents 23,9% of the total variation in the data. **(B,C)** Analysis of RNA-seq data performed with ROS-low CD34$^+$ and ROS-high CD34$^+$ cells from AML patients (n=4). **(B)** Heatmap of high-confidence genes that are downregulated in ROS-low cells compared to ROS-high cells. **(C)** Heatmap of high-confidence genes that are upregulated in in ROS-low cells compared to ROS-high cells.

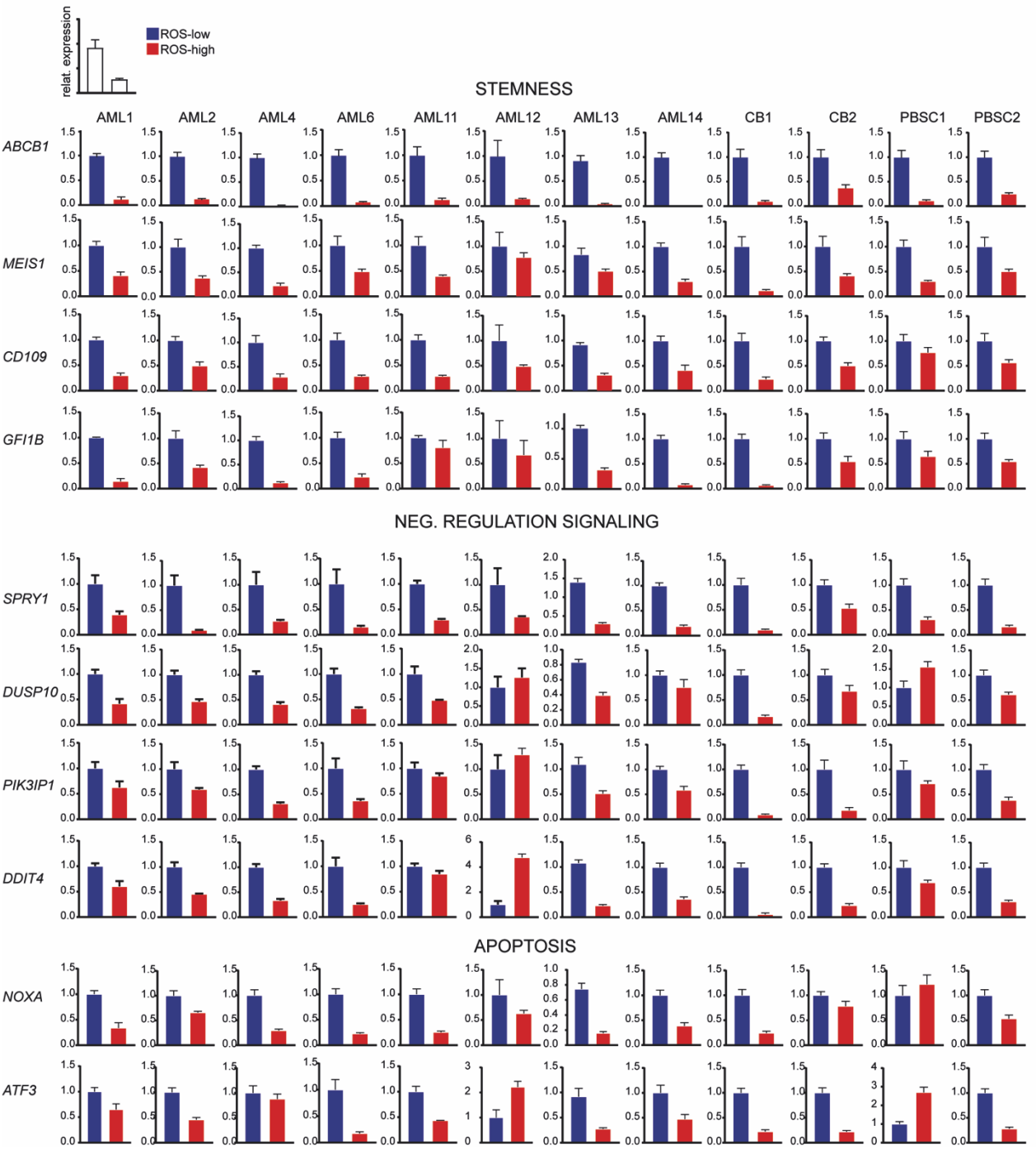

Supplementary figure 3. **ROS-low CD34$^+$ express gene signatures associated with stemness, negative regulation of signaling and apoptosis** RT-qPCR data. Relative mRNA expression of indicated genes is shown for the ROS-low and ROS-high fraction of CD34$^+$ AML cells, CD34$^+$ cord blood (CB) cells or CD34$^+$ peripheral blood stem cells (PBSCs). Error bars indicate s.d. of RT-qPCR triplicates.

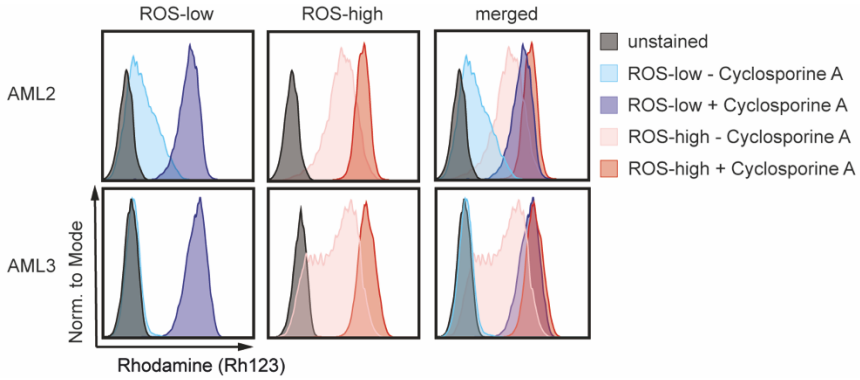

Supplementary figure 4. **ROS-low and ROS-high CD34^{+} cells show altered drug efflux transporter activity** ABCB1 transporter activity assay. FACS plots indicating signal intensities for the dye Rhodamine 123 (Rh123) are shown. Staining was performed either in the presence (+ cyclosporine A) or absence (-cyclosporine A) of the efflux transporter inhibitor cyclosporine A.

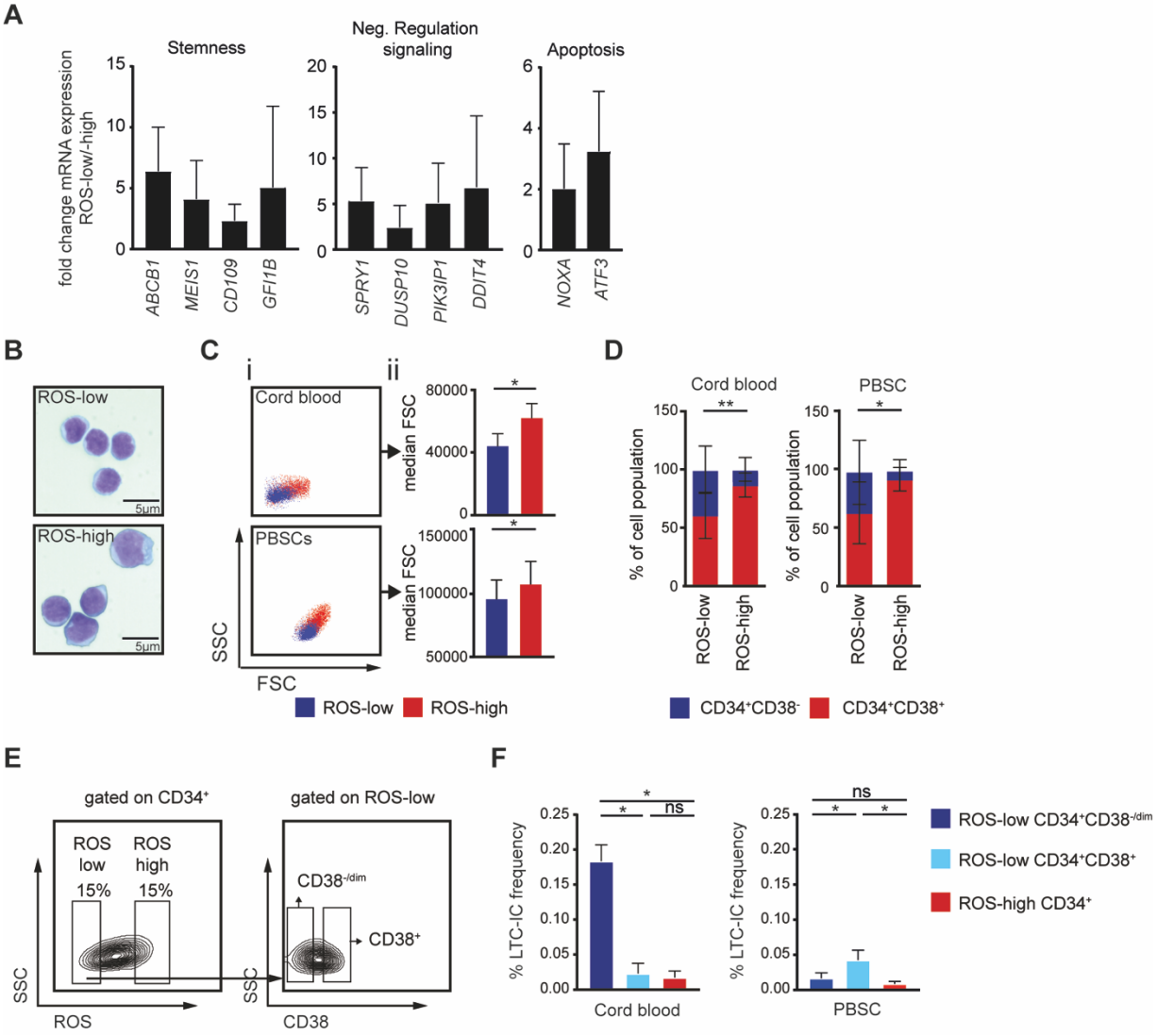

Supplementary figure 5. **Normal ROS-low CD34$^+$ have similar features compared to leukemic ROS-low CD34$^+$ (A)** mRNA expression fold change of indicated genes in the ROS-low vs the ROS-high cell fraction of normal (both CB and PBSCs) CD34$^+$ stem- and progenitor cells (n=4). Genes are assigned to the categories “stemness”, “negative regulation of signaling” and “apoptosis”. Error bars indicate s.d. **(B)** May-Grünwald Giemsa (MGG) staining of ROS-low and ROS-high sorted PBSCs. **(C) (i)** Representative FACS plots indicating the size of ROS-low (blue) and ROS-high (red) CD34$^+$ cells isolated from CB or PBSCs. **(ii)** Median forward scatter (FSC) of ROS-low and ROS-high cells from four CB donors and five PBSC donors. **(D)** Summary of FACS analysis indicating the percentages of CD38$^+$ and CD38$^-$ cell populations within ROS-low and ROS-high CD34$^+$ CB cells (n=4) or PBSCs (n=5). **(E)** Sorting strategy for LTC-IC assays. Three populations were sorted: ROS-high CD34$^+$, ROS-low CD34$^+$CD38$^{-/dim}$ and ROS-low CD34$^+$CD38$^+$.

(F) LTC-IC frequency of indicated cell populations isolated from CB (left panel; n=2; each experiment performed with a cell pool from 15-20 CB donors) or PBSCs (right panel; n=3 individual donors). **(C,D,F)** Error bars indicate s.d.; *p<0,05; **p<0.01; ns=not significant. CB: cord blood, PBSC: peripheral blood stem cells;

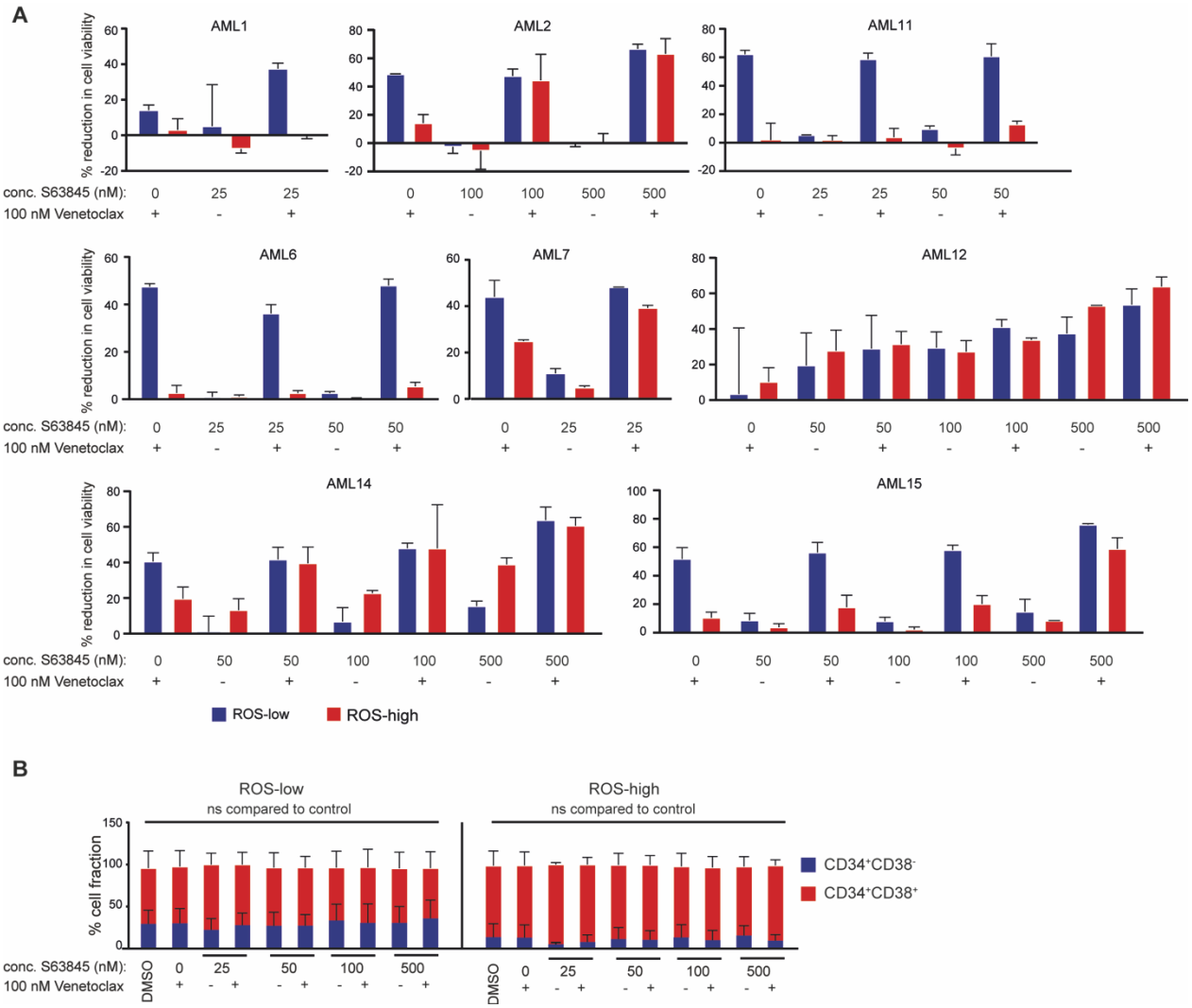

Supplementary figure 6. **CD34$^+$ AML cells with low ROS levels show an increased sensitivity to BCL2 inhibition but not to MCL1 inhibition (A)** CD34$^+$ AML cells (n=8) were sorted into ROS-low and ROS-high cell fractions and treated for 24h with 100nM Venetoclax and/or indicated concentrations of the MCL1 inhibitor S63845. Reduction of cell viability compared to control cells as indicated by DAPI staining is shown. Error bars indicate s.d. of duplicates. **(B)** Summary of FACS analysis indicating the percentages of CD34$^+$CD38$^-$ and CD34$^+$CD38$^+$ cells of control and treated cells.

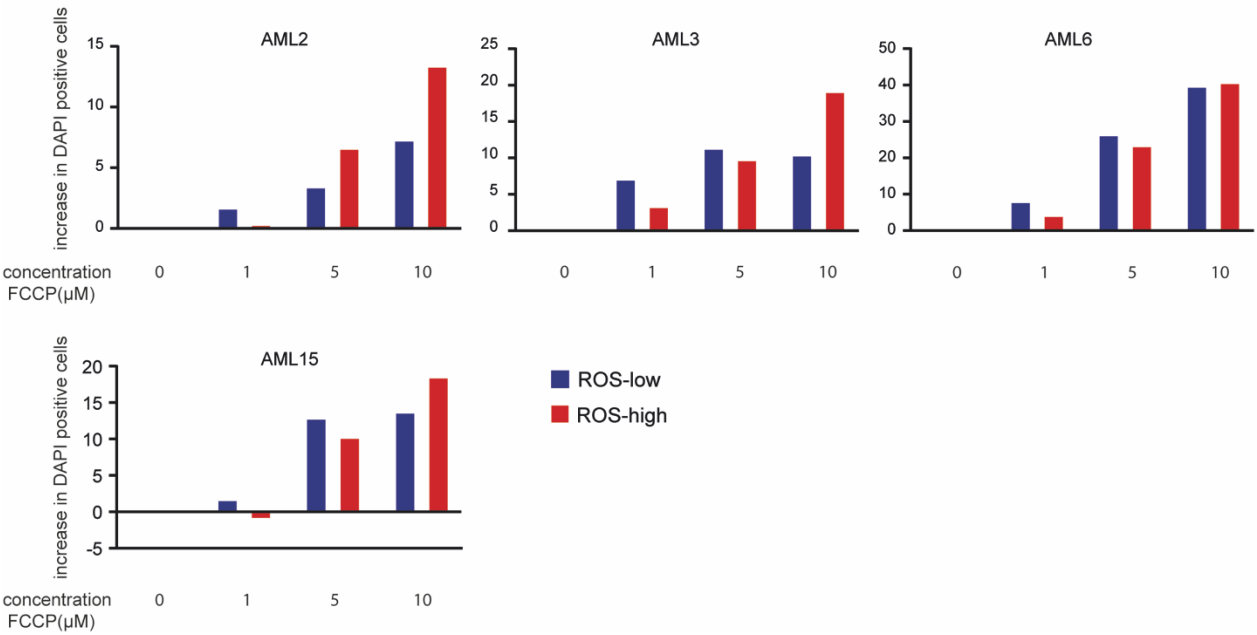

Supplementary figure 7. **FCCP mediated depolarization of the mitochondrial membrane potential targets both ROS-low and ROS-high CD34$^+$ AML cells** ROS-low and ROS-high CD34$^+$ AML cells were treated with the indicated concentrations of FCCP (carbonyl cyanide-4(trifluoromethoxy)phenylhydrazone) for 24h. The increased percentage of DAPI positive cells compared to control cells after 24h is shown.

Table S1**. Characteristics of AML patient samples used in the present study**

Clinical characteristics of the studied AML samples. If sequencing data was available, identified mutations and the variant allele frequency are indicated. All material was obtained from newly diagnosed AML patients. AML: acute myeloid leukemia; N.D: not determined.

AML ID	Age (yrs)	Cytogenetics	Molecular mutations
AML1	81	46,XX	EZH2 (97%); ASXL1 (50%); RUNX1 (98%) FLT3-ITD
AML2	70	46,XY	DNMT3A (49%); IDH2 (47%); SRSF2 (44%)
AML3	78	46,XY	TET2 (36%); EZH2 (22%); ZRSR2 (63%)
AML4	66	45,XY,-7[9]	EZH2 (89%); RUNX1 (63%) IDH1 (46%) ASXL1 (30%)
AML5	69	46,XX	NPM1mut; TET2
AML6	78	47,XY,+11[3]	IDH2 (50%); SRSF2 (49%); RUNX1 (47%)
AML7	64	47,XY,+8[3]	TET2 (30%); EZH2 (99%); FLT3-ITD (12%); RUNX1 (48%); ASXL1 (31%)
AML8	58	46,XX	NPM1mut; FLT3-ITD
AML9	35	46,XX	DNTM3A (50%); NPM1mut (40%); IDH2 (40%); FLT3-ITD (13%)
AML10	72	47,XY,+8[10]	FLT3-ITD
AML11	50	46,XY	RUNX1 (55%)
AML12	39	47,XX,+8[10]	FLT3-ITD
AML13	68	45,XX,del(5)	N.D.
AML14	50	46,XX, inv(16)(p13.1q22)	N.D.
AML15	69	45,XX,add(3)(q21),t(5;7)(q15;p21),-7	N.D
AML16	67	46,XX	FLT3-ITD
AML17	69	46,XX,t(2;3)(p25;p25)	TET2 (43%)
AML18	76	46,XY	C-kit$^+$, FLT3-ITD
AML19	74	46,XX	TET2 (36%), CEBPα (44%), DNMT3A (48%),
AML20	69	46,XX	FLT3-ITD;
AML21	74	46,XX, del(4), del(5), del(11), del(17)	SF3B1 (21%); TP53 (56%)

Material and Methods

Normal Hematopoietic cells and AML patient material

Umbilical cord blood (CB) was derived from healthy full-term pregnancies after informed consent from the Obstetrics departments of the Martini Hospital and University Medical Center Groningen (UMCG), the Netherlands. Mononuclear cells (MNCs) were isolated by density gradient centrifugation using Lymphoprep (Alere Technologies AS, Oslo, Norway) and CD34$^+$ cells were

selected using the MACS CD34 microbead kit on autoMACS (Miltenyi Biotec, Leiden, The Netherlands). A purity of >96% $CD34^+$ cells after isolation was confirmed by flow cytometry. AML blasts from peripheral blood or bone marrow from patients were studied after informed consent was obtained in accordance with the Declaration of Helsinki. The protocol was approved by the Ethical Review Board of the University Medical Center Groningen, Groningen, The Netherlands. CB $CD34^+$ cells or AML MNCs were cryopreserved in medium containing 10% fetal calf serum (FCS; Sigma, F7524) and 10% DMSO.

Preparation of primary material for subsequent analysis

Frozen material was defrosted one day prior to further analysis. CB cells were cultured overnight (o/n) in Stemline II (Sigma, Zwijndrecht, the Netherlands) supplemented with SCF, FLT-3 ligand and N-Plate (Amgen) (100 ng/ml each). AML MNCs were enriched for $CD34^+$ cells as described above, and cultured o/n on a confluent layer of murine MS5 cells in Gartner's medium consisting of αMEM (containing glutamine, Lonza) supplemented with 12.5 % heat-inactivated FCS (Sigma), 12.5 % heat-inactivated horse serum (Sigma), 100 U/mL penicillin and streptomycin (PAA Laboratories), 57.2 μM β-mercaptoethanol (Merck Sharp & Dohme BV), 1 mM hydrocortisone (Sigma) and 20 ng/mL G-SCF, N-Plate and IL-3. MS5 cells were cultured and maintained as described previously.[1]

Cell separation based on ROS levels

Normal – or leukemic $CD34^+$ cells, prepared as described above, were resuspended in PBS/3%FCS/Fc-block and stained with 5 μM CellROX Deep Red reagent (Life Technologies) and antibodies for CD34/CD38 selection (CD34-PE, CD38-FITC, both BD Biosciences) for 30 min at 37 °C. Afterwards, cells were washed with PBS/3%FCS and resuspended in PBS/3%FCS containing 10 μM DAPI. Labelled cells were further analyzed using LSR II (BD Biosciences) and FlowJo software (Treestar), or sorted on MoFLo XDP or Astrios (DakoCytomation, Carpinteria, CA, USA). For cell sorting, viable $CD34^+$ cells with the 15 % lowest – and 15 % highest signal intensity for the ROS-dye were collected.

Long-term Culture-Initiating Cell (LTC-IC) assay

ROS-low and ROS-high sorted $CD34^+$ CB cells or PBSCs were plated in limiting dilutions in the range of 9 to 1000 cells per well on MS5 stromal cells in 96-well plates in LTC medium (Glutamine containing αMEM supplemented with heat-inactivated 12.5% FCS, heat-inactivated 12.5% horse serum (Sigma), 100 U/mL penicillin/streptomycin (PAA Laboratories), 57.2 μM β-mercaptoethanol

(Merck Sharp & Dohme BV) and 1 µM hydrocortisone (Sigma)). After 5 weeks, methylcellulose (MethoCult H4230, Stemcell Technologies) supplemented with 19% (v/v) IMDM, 100 U/mL penicillin/streptomycin, 20 ng/mL IL-3, 20 ng/mL IL-6, 20 ng/mL G-CSF, 20 ng/mL SCF and 1 U/mL EPO was added to the wells. Two weeks later, wells containing colony forming cells (CFCs) were scored as positive. LTC-IC frequency was calculated using the L-Calc software.

Immunoblotting

Preparation of cell lysates and immunoblotting procedure was performed as described previously.[2] Primary antibodies for immunoblotting were: BCL2 (2872, Cell Signaling), TOM20 (D8T4N, 42406, Cell Signaling), HDAC1 (10E2, 5356, Cell Signaling), β-ACTIN (C4, SC-47778, Santa Cruz).

ABCB1 transporter activity assay

Sorted $CD34^+$ AML cells were divided in two tubes and resuspended in either 1 ml of αMEM or in 1 ml of αMEM + 4 µM cyclosporine A (CSA) (Sigma, #C3663). Rhodamine 123 (Dojindo Laboratories, via Tebu-bio) was added to a final concentration of 200 ng/ml and cells were incubated for 20 min at 37^0C. Afterwards, cells were washed 2x with ice cold αMEM, resuspended in αMEM with or without addition of CSA, and incubated for 1h at 37^0C. Subsequently, cells were washed 2x with ice cold PBS/FCS, resuspended in PBS/FCS/DAPI and analyzed on LSR II. The transporter activity was defined as the difference in Rhodamine 123 signal intensity between the fractions with and without the efflux pump inhibitor CSA (Transporter activity = MFI (-CSA)/MFI (+CSA)), as described previously.[3]

RNA Extraction and Illumina high-throughput sequencing

RNA was isolated by separation of the aqueous phase by TRIzol Reagent (Thermo Fisher) according to the manufactures protocol. The aqueous phase was mixed with 70% ethanol (1:1) and isolation was continued using the RNeasy micro kit (Qiagen) including on-column DNaseI treatment. RNA libraries were prepared using the KAPA RNA HyperPrep Kit with RiboErase (HMR) according to the manufactures protocol (KR1351 – v1.16, Roche Sequencing Solutions). In brief: 25ng -1ug input RNA was depleted from ribosomal RNA by oligo hybridization, RNaseH treatment and DNase digestion. rRNA-depleted RNA was fragmented to ~200 bp fragments and first strand synthesis was performed using random primers. The second-strand was synthesized using dUTP for strand specificity. After adapter ligation, library amplification was performed and the number of cycles was dependent on the amount of starting material. A bioanalyser with a high

sensitivity DNA Chip (Agilent) was used to check fragment size. Samples were sequenced on an Illumina NextSeq 500 system with 2×43 bp paired-end sequencing (PE43).

RNA-Sequencing analysis

STAR aligner with UCSC gene annotation first indexed the hg19 reference genome. The resulting RNA-seq reads were mapped to the hg19 genome using STAR with two-pass mode, and the gene-level read counts were enumerated at the same time. EdgeR (v3.24.3) was used to examine differentially expressed genes and genes with ≥1log difference and adj p-value of <0.01 were considered significant. EdgeR analysis was overlapped with genes that have > 1.5 fold difference in all samples in a pairwise comparison. Raw RNA-Sequencing data are available at http://www.ncbi.nlm.nih.gov/geo, with accession code: GSE131422. GO-analysis was performed with metascape (www.metascape.org).

Mitochondrial copy number assay

Total DNA was isolated from >1 x10^5 cells using QIAamp DNA mini kit (Qiagen). DNA was amplified real-time in SYBR Green Supermix (Bio-Rad) using the CFX connect Thermocycler (Bio-Rad). Nuclear genes (GAPDH and B2M) and mitochondrial genes (12S and tRNA) were amplified using the following primers:

Gene	Forward primer	Reverse primer
B2M	5'- TGCTGTCTCCATGTTTGATGTATCT -3'	5'- TCTCTGCTCCCCACCTCTAAGT -3'
GAPDH	5'- TACTGGTGTCTTCACCACCA -3'	5'- CAGGATGCATTGCTGACAATC -3'
12sRNA	5'- AGAACACTACGAGCCACAGC -3'	5'- ACTTGCGCTTACTTTGTAGCC -3'
tRNA-Leu	5'- CACCCAAGAACAGGGTTTGT -3'	5'- TGGCCATGGGTATGTTGTTA -3'

The obtained CT values were corrected for the corresponding calculated primer reaction efficiencies. Based on the corrected CT values, the mitochondrial DNA copy number was calculated relative to nuclear DNA copy number.[4]

ATP assay

Luminescent ATP detection Assay kit (Abcam, ab113849) was used according to the manufactures protocol to measure levels of ATP. ATP levels were measured using a Bio-Rad benchmark III Bio-Rad microtiter spectrophotometer.

Mutational analysis and targeted sequencing

Presence of the FLT-ITD mutation was analyzed by PCR using following primers: FLT3-ITD_fw: CGGCACAGCCCAGTAAAGATA; FLT3-ITD_rev: GCCCAAGGACAGATGTGATG; The NPM1 region was amplified using following primers: NPM1_W288fs_fw: TCGGGAGATGAAGTTGGAAG and NPM1_W288fs_rev: ACGGTAGGGAAAGTTCTCAC, and presence of the mutation was verified by Sanger-Sequencing (Eurofins).

Ultrastructural analysis

The experimental procedure for ultrastructural analysis of hematopoietic cells has been described previously.[5] In brief, 1-2 million ROS-low and ROS-high sorted $CD34^+$ AML cells were pelleted and subsequently fixed in 2% paraformaldehyde and 2% glutaraldehyde in 0.1M cacodyladate buffer for 24h at 4 °C. After fixation, the cells were washed in in 0.1M cacodyladate buffer. Cells were stained with Evans blue and subsequently embedded in low melting point agarose as described previously.[6] Agarose pieces containing the cell pellet were dehydrated, osmicated, and embedded in Epon according to routine procedures. Semi-thin sections (0.5mm) stained with toluidine blue were inspected using light microscopy to identify the position of cells. Ultra-thin sections (60-80 nm) were cut and stained with 4% uranyl acetate in water, followed by Reynolds lead citrate. Images were taken with the FEI/Philips CM100 (Eindhoven, the Netherlands).

Measurement mitochondrial structures and cytoplasm area

Electron microscopy images of ROS-low and ROS-high sorted $CD34^+$ AML cells were taken as described above. On these images, mitochondrial structures were counted from 25-70 cells per sample. Similar, the cytoplasm area of 25-70 cells per sample was outlined and measured using ImageJ. To report the relation between cell size and mitochondrial content, the ratio of the average cytoplasm area and the average number of mitochondrial structures per sample was calculated.

Analysis of cell viability after drug treatment

ROS-low and ROS-high $CD34^+$ AML cells were sorted as described above and resuspended in αMEM (containing glutamine) supplemented with 20 % heat-inactivated FCS, 100 U/mL penicillin and streptomycin, and 20 ng/mL G-SCF, N-Plate and IL-3. Afterwards, cells were treated with either DMSO (served as control), 100 nM of the BCL2 inhibitor Venetoclax (Selleckchem), or various concentrations of the MCL1 inhibitor S63845 (APExBIO). After 24h, the cell viability was determined by DAPI staining with subsequent FACS analysis. For Figure 3 B-D, the effect of drug treatment was presented as the percentage of cell viability reduction compared to DMSO-treated control cells.

Statistics

If not indicated in the figure legends otherwise, the paired two-sided student's t-test was used to calculate statistical differences between the ROS-low and ROS-high cell fractions. A p-value of <0.05 was considered statistically significant.

References

1. Schepers H, van Gosliga D, Wierenga ATJ, Eggen BJL, Schuringa JJ, Vellenga E. STAT5 is required for long-term maintenance of normal and leukemic human stem/progenitor cells. Blood 2007;110(8):2880–2888.

2. Mattes K, Berger G, Geugien M, Vellenga E, Schepers H. CITED2 affects leukemic cell survival by interfering with p53 activation. Cell Death Dis 2017;8(10):e3132.

3. Broxterman HJ, Sonneveld P, Feller N, et al. Quality control of multidrug resistance assays in adult acute leukemia: correlation between assays for P-glycoprotein expression and activity. Blood 1996;87(11):4809–4816.

4. Rooney JP, Ryde IT, Sanders LH, et al. PCR based determination of mitochondrial DNA copy number in multiple species. Methods Mol Biol 2015;124123–38.

5. Houwerzijl EJ, Blom NR, van der Want JJL, et al. Increased peripheral platelet destruction and caspase-3-independent programmed cell death of bone marrow megakaryocytes in myelodysplastic patients. Blood 2005;105(9):3472–3479.

6. Kumar S, Ciraolo G, Hinge A, Filippi M-D. An efficient and reproducible process for transmission electron microscopy (TEM) of rare cell populations. J Immunol Methods 2014;40487–90.